

Phase transition of a Pb monolayer on Ge(111)

S. A. de Vries and P. Goettkindt*

FOM-Institute for Atomic and Molecular Physics, Kruislaan 407, 1098 SJ Amsterdam, The Netherlands

P. Steadman*

Department of Physics and Astronomy, University of Leicester, Leicester LE1 7RH, United Kingdom

E. Vlieg[†]

*FOM-Institute for Atomic and Molecular Physics, Kruislaan 407, 1098 SJ Amsterdam, The Netherlands
and RIM, Department of Solid State Chemistry, University of Nijmegen, Toernooiveld 1, 6525 ED Nijmegen, The Netherlands*

(Received 15 January 1999)

We present an x-ray-diffraction structural analysis of the β -Ge(111)- $(\sqrt{3} \times \sqrt{3})R30^\circ$ -Pb $\rightarrow 1 \times 1$ phase transition at $\sim 180^\circ\text{C}$ for a Pb coverage of 1.25 ML. We have studied the atomic structure below and above the phase transition by measuring the distribution of diffracted intensities along integer-order rods of Bragg scattering. Below the phase transition, the β phase has a saturation coverage of $\frac{4}{3}$ ML. We find that above the phase transition the single layer of Pb gives rise to a ring of diffuse scattering indicative of a two-dimensional liquid. However, of all the Pb geometries considered, an ordered layer with high in-plane thermal vibration amplitude is found to provide the best agreement between calculated and measured structure factors. The Pb layer thus has both liquid and solid properties. [S0163-1829(99)08019-4]

I. INTRODUCTION

Solid-liquid interfaces are found in many areas, but atomic-scale experimental data are scarce. Ultrathin liquid boundary layers are thought to affect properties such as flow, lubrication, and wear. Little is known about the interaction of liquid metals with solid surfaces in processes such as casting, molding of steel and alloys, soldering, welding, and sintering. In the process of liquid-phase epitaxial growth, semiconductor surfaces are in contact with liquid metals.¹ Most theoretical predictions on the liquid ordering at solid-liquid interfaces have not been verified experimentally.

Liquid ordering in two dimensions is also of great fundamental interest.² Most experiments on two-dimensional systems are not on a free layer of atoms, but consist of a two-dimensional layer supported by a substrate. An important question in these systems is how the periodicity of the ad-layer is related to the periodicity of the substrate. The solid-liquid interface that occurs during surface melting³ is of equal fundamental interest, but here also the precise structure of the liquid remains unknown.^{4,5}

Pb monolayers adsorbed on Ge surfaces constitute an ideal two-dimensional metal. Since the mutual solid solubilities are negligible over all temperatures for which lead does not desorb, a well-defined interface is formed, without complications due to alloying or dissolution in the bulk. The Pb can be easily removed and deposited again. Like most semiconductor interfaces, the Pb/Ge(111) system shows interesting atomic and electronic structures and it has therefore been the subject of numerous investigations.⁶⁻²⁹ Here we focus on the disordering transition of a $(\sqrt{3} \times \sqrt{3})R30^\circ$ reconstruction to a 1×1 phase at $\sim 180^\circ\text{C}$.

Before studying a phase transition of an adsorbed layer, one should know the exact atomic structure of the phases above and below the transition. As a function of coverage

there are two different room temperature $(\sqrt{3} \times \sqrt{3})R30^\circ$ structures on Ge(111): a dilute α phase and a dense β phase; see Fig. 1. The α phase has a coverage of $\frac{1}{3}$ ML, where 1 ML is defined as one chemisorbed atom per top layer Ge atom of the unreconstructed, ideal Ge(111). The α phase is well understood and consists of one atom per $(\sqrt{3} \times \sqrt{3})R30^\circ$ unit cell chemisorbed on a T_4 site on top of the second layer of Ge.^{9,11,12,16} The coverage and structure of the dense β phase, however, has been debated for many years.

The main controversy about the β phase is the saturation coverage. From reflection high-energy electron-diffraction (RHEED), x-ray scattering, and low-energy electron-diffraction (LEED) measurements, a structural model has been proposed with a saturation coverage of $\frac{4}{3}$ ML (four atoms per unit cell).^{7-9,14-16,26} This structure is essentially a 1% compressed close-packed Pb(111) layer rotated by 30° with respect to the underlying Ge lattice. Per unit cell, three Pb atoms occupy the bridge sites between T_4 and T_1 sites, with a small displacement to the T_1 sites [therefore also called off-centered (OC) T_1 sites], and one atom occupies an H_3 site. Scanning tunneling microscopy (STM) experiments are consistent with a $\frac{4}{3}$ -ML structure, but here the Pb atoms were thought to be on OC T_4 sites.²⁰ The $\frac{4}{3}$ -ML saturation coverage was also found in a first-principles molecular dynamics study, where a ‘‘chain’’ model has been proposed.¹⁹

Other LEED and STM measurements have reported that the saturation coverage for the β phase is 1 ML (three atoms per unit cell).^{6,21,22} Hwang and Golovchenko²¹ derived this coverage with Rutherford backscattering. They proposed a model consisting of three Pb atoms per unit cell, which are displaced from the T_1 sites to form trimers around the H_3 sites of the Ge substrate. First-principles calculations find that this trimer structure at 1-ML coverage is unstable.¹⁹ An overview of the different models proposed is given by-

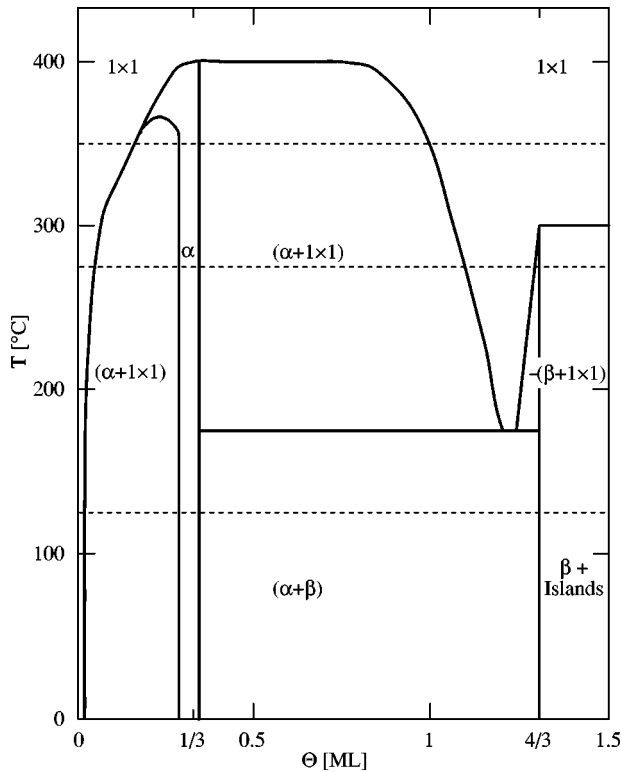


FIG. 1. Phase diagram of Pb/Ge(111) proposed by Grey (Ref. 13). The dashed lines mark the different temperatures at which we monitored the fractional-order ($\frac{2}{3}$ $\frac{2}{3}$ 0.1) reflection during Pb deposition (see Fig. 2).

Franklin *et al.*,²⁶ from which we can conclude that most evidence points to a $\frac{4}{3}$ -ML saturation coverage.

Using RHEED, Ichikawa^{7,8} was the first to derive a phase diagram for Pb/Ge(111). Ichikawa reported that a Pb monolayer on the Ge(111) surface undergoes a solid-to-liquid phase transition at a temperature which depends critically on the coverage going from 192 to 333 °C. This phase transition was thought to correspond to the melting of the Pb monolayer. Using LEED, Métois and Le Lay⁶ found a reversible ($\sqrt{3} \times \sqrt{3}$)R30° to 1×1 transition at 280 °C, which they claimed is not an order-disorder transition, because of the sharpness of their 1×1 LEED pattern at 300 °C. LEED did not show any rings of diffuse scattering. Therefore, Métois and Le Lay described it as a solid-solid structure change.

A thorough investigation of the phase diagram was done by Grey,¹³ showing that below a coverage of $\frac{4}{3}$ ML a low-temperature phase transition to the 1×1 phase occurs around ~180 °C. Above $\frac{4}{3}$ ML a high-temperature phase transition occurs around ~330 °C. For convenience, the phase diagram proposed by Grey is shown in Fig. 1.

Grey *et al.*¹⁷ studied the phase transition from the β -($\sqrt{3} \times \sqrt{3}$)R30° phase to the 1×1 phase at a temperature of 180 °C and a coverage of 1.25 ML. From their experimental x-ray observation of a diffraction ring, they concluded that the Pb forms a two-dimensional, modulated liquid. However, Hwang and Golovchenko^{21,22} proposed an alternative explanation for this phase on the basis of STM observations. They claimed that the β phase breaks up into very small domains at the transition temperature of 180 °C with the Pb atoms in a state of greatly agitated motion.

In order to resolve this controversy, we have measured the intensity along crystal truncation rods (CTR's)³⁰ above and below the phase transition. These rods are tails of diffuse intensity connecting the bulk Bragg peaks in the direction perpendicular to the surface. The intensity along a CTR is given by the interference sum of the bulk and surface contributions. Such integer-order positions in reciprocal space are insensitive to the antiphase disorder that Hwang and Golovchenko claimed to be the origin of the phase transition at ~180 °C. If at this temperature only the domain size is changing, no change in the CTR intensity is expected. On the other hand, a transition to a two-dimensional liquid should have a profound effect on the CTR's.

II. EXPERIMENT

The x-ray-diffraction measurements were performed at station 9.4 of the Synchrotron Radiation Source, Daresbury Laboratory, United Kingdom.³¹ Monochromatic x rays with a wavelength λ of 0.92 Å (13.5 keV) were used, with both the primary and diffracted beams collimated by slits. All data were taken with a constant outgoing angle of 1° and varying incoming angles, thereby keeping the detector resolution constant. The sample was mounted in an ultrahigh-vacuum chamber³² coupled to a five-circle diffractometer.³³ A Knudsen effusion cell was used for Pb deposition at a rate of ~0.003 ML/sec.

The polished single crystal Ge(111) sample ($8 \times 8 \times 2$ mm³) had a miscut smaller than 0.1°. The sample was cleaned by repeated cycles of sputtering (600-eV Ar⁺, 10 μ A min) and annealing (700 °C for 15 min). Ge has a diamond-type lattice which has an ABC stacking of bilayers along the $\langle 111 \rangle$ direction. Expressed in conventional cubic lattice vectors, the primitive lattice vectors $\{a_i\}$ spanning the surface unit cell are given by

$$\mathbf{a}_1 = \frac{1}{2} [1 \ 0 \ \bar{1}]_{\text{cubic}}, \quad \mathbf{a}_2 = \frac{1}{2} [\bar{1} \ 1 \ 0]_{\text{cubic}}, \quad \mathbf{a}_3 = [1 \ 1 \ 1]_{\text{cubic}}, \quad (1)$$

with

$$|\mathbf{a}_1| = |\mathbf{a}_2| = \frac{1}{2} \sqrt{2} a_0, \quad |\mathbf{a}_3| = \sqrt{3} a_0,$$

and a_0 the lattice constant of bulk Ge (5.658 Å). The corresponding reciprocal-lattice vectors $\{\mathbf{b}_i\}$ are defined by $\mathbf{a}_i \cdot \mathbf{b}_j = 2\pi \delta_{ij}$.

The momentum-transfer vector \mathbf{Q} is the difference between the outgoing wave vector \mathbf{k}_{out} and the incoming wave vector \mathbf{k}_{in} ($|\mathbf{k}_{\text{out}}| = |\mathbf{k}_{\text{in}}| = 2\pi/\lambda$), and is denoted by diffraction indices (hkl) in reciprocal space:

$$\mathbf{Q} = h\mathbf{b}_1 + k\mathbf{b}_2 + l\mathbf{b}_3. \quad (2)$$

Here the diffraction-index pair (hk) refers to the in-plane component, and the index l to the perpendicular component of \mathbf{Q} . For CTR's, which are labeled by (hk), the indices h and k have integer values, whereas l is unconstrained.

Integrated intensities at various values of l along a diffraction rod are determined by rotating the crystal about the surface normal and measuring the number of diffracted photons. Structure factors are obtained by dividing the measured in-

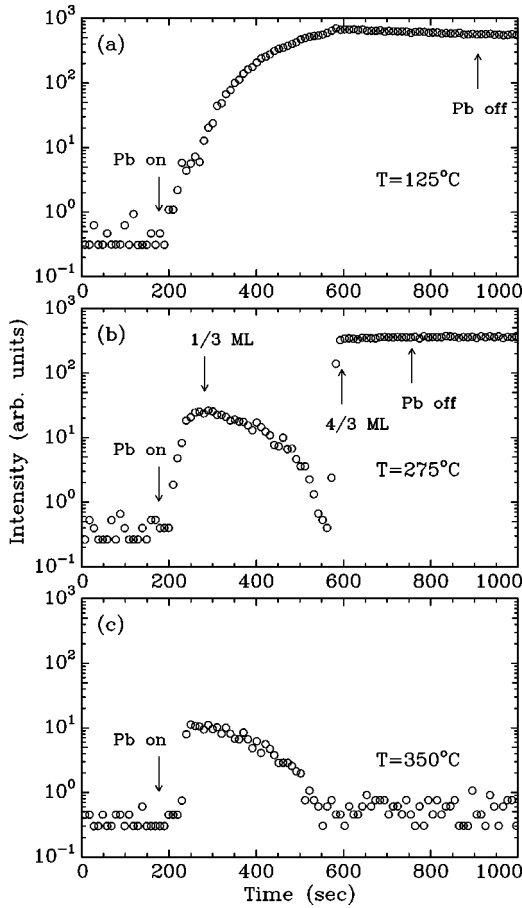


FIG. 2. The $(hkl) = (\frac{2}{3} \frac{2}{3} 0.1)$ fractional-order reflection during Pb deposition at three different Ge(111) substrate temperatures. The arrows indicate the starting and stopping of the Pb deposition. In (b), the completion of the α phase after 105 sec of deposition ($\frac{1}{3}$ ML), and the β phase after 420 sec ($\frac{4}{3}$ ML), are indicated by arrows as well.

tensity by the Lorentz factor, the polarization factor, and an area correction factor, and taking the square root.³⁴ The area correction factor for the variation of the x-ray footprint on the sample is calculated numerically by assuming a Gaussian beam profile with a full width at half maximum (FWHM) of 2.1 mm in the horizontal direction and 1.6 mm in the vertical direction. The error in the individual structure factors was determined from the counting statistics. Symmetry-equivalent reflections were measured as well, from which an estimate for the systematic error was derived,³⁵ varying between 7 and 12% for the different data sets.

III. RESULTS AND DISCUSSION

A. Saturation coverage of the β phase

First we investigate the deposition of Pb on Ge(111). In Fig. 2 the intensity of the $(hkl) = (\frac{2}{3} \frac{2}{3} 0.1)$ fractional-order reflection that is sensitive to the $(\sqrt{3} \times \sqrt{3})R30^\circ$ structure is shown during Pb deposition at three different substrate temperatures. These curves (marked by the dashed lines in Fig. 1) beautifully confirm the phase diagram as proposed by Grey.¹³ At a substrate temperature of 125 °C [Fig. 2(a)], well below the low-temperature phase transition, the intensity

rises constantly after starting the Pb deposition. First the α phase is formed. After a deposition of $\frac{1}{3}$ ML this phase is completed and the β phase starts to form as well. Both phases have a $(\sqrt{3} \times \sqrt{3})R30^\circ$ structure, and therefore the transition from one to the other is not visible in this scan. Because of both the strong scattering of Pb atoms (compare $Z_{\text{Pb}}=82$ and $Z_{\text{Ge}}=32$) and the increase in domain size, the intensity rises quite dramatically. After the deposition we made a transverse in-plane scan of the $(\frac{2}{3} \frac{2}{3} 0.1)$ reflection. By measuring the peak full width at half maximum ΔQ_{FWHM} we can derive the correlation length $L=2/\Delta Q_{\text{FWHM}}$.³⁶ For deposition at 125 °C we find a correlation length of 1650 Å.

In Fig. 2(b), the same experiment is shown for a substrate temperature of 275 °C, which is well above the low-temperature phase transition. From the intensity it is clear at which moment the α and β phases are complete. First the intensity rises when the α phase is formed. Since the α phase is known to be completed after deposition of $\frac{1}{3}$ ML, we can estimate from this figure at which moment we have deposited $\frac{1}{3}$ ML. The arrow indicates this position, which is after 105 sec. After exactly four times this amount, 420 sec, the β phase is completed (second arrow). In between the intensity goes back to zero, because of the low-temperature phase transition around 180 °C for a coverage just below $\frac{4}{3}$ ML. Assuming that no desorption occurs, the β phase thus has a saturation coverage of $\frac{4}{3}$ ML. From Fig. 2(b) it becomes clear that the phase transition to the 1×1 phase critically depends on the coverage. Below $\frac{4}{3}$ ML it occurs around $\sim 180^\circ\text{C}$, and above $\frac{4}{3}$ ML around 300 °C. Also here we measured a transverse in-plane scan of the $(\frac{2}{3} \frac{2}{3} 0.1)$ reflection, for which we found a resolution limited $\Delta Q_{\text{FWHM}} \cong 0.7 \times 10^{-3} \text{ \AA}^{-1}$, which means the correlation length is larger than 2500 Å. The domains are thus exceptionally large. Note that the completion of the β phase coincides exactly with the break in the deposition curve shown in Fig. 2(a).

Pb deposition at 350 °C is shown in Fig. 2(c). Only the α phase is formed, because we are above the high-temperature phase transition. In the remainder of this paper, we will look at the atomic structure of 1.25 ML of Pb below and above the phase transition at $\sim 180^\circ\text{C}$. The β phase is studied at a temperature of 125 °C and the 1×1 phase at 260 °C. Note that the temperature values used here are not very accurate (the absolute error is about 50 °C), but that we can reproducibly locate the phase transitions with the help of Fig. 2.

B. Atomic structure of the β phase

In order to determine the atomic structure below and above the phase transition we measured two integer-order CTR's, as well as a number of in-plane reflections. As a reference we measured these rods for the clean starting sample at room temperature as well. The clean Ge(111)- $c(2 \times 8)$ reconstruction has been studied before with surface x-ray diffraction.^{37,38} Our data is consistent with the structural model of Van Silfhout *et al.*³⁸

In Fig. 3 the measured structure factor amplitudes for the β phase along the (01) and (02) CTR's are shown together with model calculations as a function of perpendicular momentum transfer l , expressed in reciprocal-lattice units. We

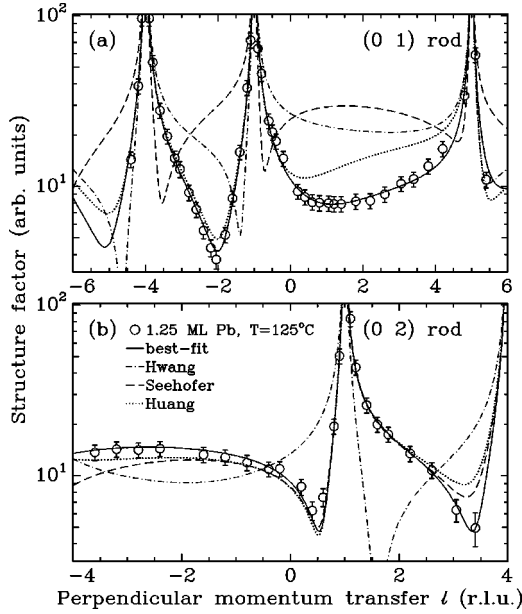


FIG. 3. Structure factor amplitudes along the $(hk)=(0\ 1)$ and $(0\ 2)$ crystal truncation rods. Measured structure factors are indicated by open circles. The solid curve represents our best-fit model calculation. For comparison calculations for the models proposed in Refs. 21 (dash-dotted line), 20 (dashed line), and 16 (dotted line) are also shown.

have started our analysis with the model proposed by Feidenhans'l *et al.*,⁹ where one Pb atom is placed on an H_3 site, and the other three Pb atoms on the bridge sites between the T_1 and T_4 sites. One fitting parameter is used to allow these three atoms to move off-center to the T_1 or T_4 site. For the height of the Pb atoms, two fitting parameters were used for the two different sites (H_3 and bridge sites). With a global scaling parameter, a surface fraction parameter θ (fraction of surface that adopts the model surface structure), and in-plane and out-of-plane Debye-Waller parameters B_{par} and B_{perp} for the Pb atoms, the total number of free fitting parameters used in our χ^2 minimization was 7. For the Ge atoms an isotropic Debye-Waller B parameter was fixed at the room temperature bulk value of $0.58\ \text{\AA}^2$.³⁹ All Ge atoms were fixed at bulk positions, because no significant improvement to the fit was found by allowing them to relax. The best fit has a reduced χ^2 value of 1.3.

A schematic of the model structure is shown in Fig. 4 in (a) top and (b) side views. One Pb atom is positioned at an H_3 site, and three atoms are displaced from the bridge site toward the T_1 sites, as indicated by the arrows. In (b) the distances between atoms and the Pb (covalent) radius are drawn to scale.

The solid curves in Fig. 3 show our best-fit model calculation. The fit parameters are shown in Table I together with the atomic coordinates. From the surface fraction parameter θ we find a coverage of $0.89 \times \frac{4}{3} = 1.19$ ML, which is close to our estimated deposition of 1.25 ML. Since the coverage is below $\frac{4}{3}$ ML, it could be that one of the sites is less occupied. However, by taking a surface fraction 1 and fitting the occupancies of the H_3 and OC T_1 sites, the reduced χ^2 went up from 1.3 to 1.8. Thus the $(\sqrt{3} \times \sqrt{3})R30^\circ$ domains appear to have locally a coverage of $\frac{4}{3}$ ML.

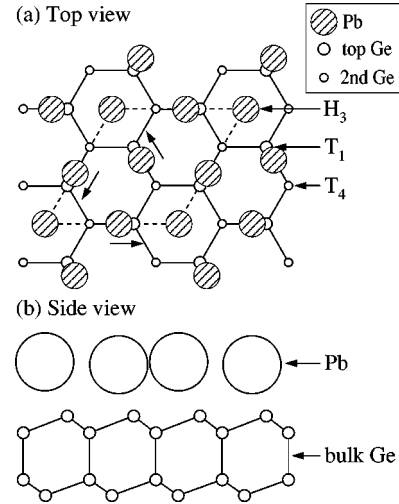


FIG. 4. Schematic projections of our structural model in (a) top view and (b) side view. The $(\sqrt{3} \times \sqrt{3})R30^\circ$ unit cell is indicated by the dashed lines. One Pb atom is positioned at an H_3 site, and three atoms are displaced from the bridge site towards the T_1 sites, as indicated by the arrows. In (b) the distances between atoms and the Pb (covalent) radius are drawn to scale.

We find that the bridge atoms are displaced toward the T_1 site (OC T_1) by an amount of $0.39\ \text{\AA}$ from the bridge center, in agreement with earlier x-ray ($0.35\ \text{\AA}$) and LEED measurements ($0.43\ \text{\AA}$).^{9,16} We find a large in-plane Debye-Waller factor of 6.3. The parameter B is related to the mean-square thermal vibration amplitude $\langle u^2 \rangle$ by $B = 8\pi^2 \langle u^2 \rangle$. We thus have an in-plane root-mean-squared thermal vibration amplitude of $0.28\ \text{\AA}$. The perpendicular Debye-Waller parameter remains small, but our fit is not significantly affected by this parameter. The total amplitude $\langle u^2 \rangle = \langle u_{\text{par}}^2 \rangle + \langle u_{\text{perp}}^2 \rangle$ corresponds to a Debye temperature of the Pb monolayer $T_D \sim 55\ \text{K}$.⁴⁰ The bulk Pb Debye temperature is $T_D = 81\ \text{K}$.

TABLE I. Best-fit parameters and atomic coordinates for the structural model for the β phase. The atom positions in the surface unit cell are given by $\mathbf{r} = x\mathbf{a}_1 + y\mathbf{a}_2 + z\mathbf{a}_3$, with $\{\mathbf{a}_i\}$ the fundamental translation vectors as defined in Eq. (1). Fixed values are indicated by an asterisk (*).

Fit parameter			
θ surface fraction	0.89(2)		
OC T_1 displacement (\AA)	0.39(4)		
Height H_3 atom (\AA)	2.88(17)		
Height OC T_1 atoms (\AA)	2.76(4)		
Debye-Waller B_{par} (\AA^2)	6.3		
Debye-Waller B_{perp} (\AA^2)	1		
Atom	x	y	z
H_3 Pb	0.333*	0.667*	0.377
OC T_1 Pb	-0.223	1.223	0.365
OC T_1 Pb	1.447	1.223	0.365
OC T_1 Pb	0.777	1.554	0.365
Top Ge	0.667*	0.333*	0.083*
2nd Ge	0.000*	0.000*	0.000*

Even lower values, however, for a Pb monolayer were found by photoemission measurements ($T_D=41$ K),¹⁰ x-ray standing-wave measurements ($T_D=32$ K),²⁶ and predicted by molecular dynamics ($T_D=34$ K).²³

There has been some debate about the height of the overlayer Pb atoms with respect to the top layer Ge atoms.⁴¹ For these vertical distances Huang *et al.*¹⁶ found 2.22 Å and 2.70 Å for the lower (at H_3) and upper (between T_1 and T_4) Pb layers, respectively. Dev *et al.*¹⁴ found 1.55 and 2.85 Å for these values. In our analysis these distances are 2.88 and 2.76 Å. So in our determination the atoms on the H_3 sites are the upper atoms. This was also found in Ref. 20, whose authors estimated the relative height difference between the H_3 and OC T_1 to be 0.15 Å, which comes close to our value of 0.12 Å. However, our error bar on the height of the H_3 atom is rather large (0.17 Å), so we cannot be very definitive about this issue. In *ab initio* molecular-dynamics calculations¹⁹ it was found that the Pb atoms all have about the same height, ~ 2.7 Å above the Ge surface.

In earlier x-ray measurements no out-of-plane positions were given,⁹ but our in-plane atomic coordinates are in agreement with these measurements as well as with the LEED measurements of Huang *et al.*¹⁶ As mentioned above, however, our model gives other height parameters for the Pb atoms. The dotted line in Fig. 3 shows a calculation for the model of Huang *et al.* Especially for the positive part of the (0 1) CTR the predicted distribution differs significantly from our measured structure factors. The model proposed in Ref. 20 agrees with ours on the out-of-plane coordinates, but differs in the way the bridge atoms are placed. In the model of Ref. 20 these Pb atoms occupy OC T_4 sites, instead of OC T_1 sites. This corresponds to changing the sign of the in-plane displacement in our model. Then we obtain the dashed curve, which is clearly not consistent with our data. From our measurements shown in Fig. 2, we have already concluded that models favoring three atoms per unit cell can be excluded. From our CTR measurements this is confirmed when we compare our data with the model proposed by Hwang and Golovchenko,²¹ that consists of a trimer with the T_1 Pb atoms displaced towards the H_3 sites by 0.3 Å (dash-dotted curve).

The models of Seehofer and of Hwang and Golovchenko are based on STM measurements. In a later paper, Seehofer *et al.*²⁵ demonstrated that the β phase has a rather complex appearance in STM images that depends on both the bias voltage and the tunneling current. Depending on the tunneling parameters they observed one, three, or four protrusions per $(\sqrt{3}\times\sqrt{3})R30^\circ$ unit cell. By comparing the results with the closely related incommensurate phase at a slightly higher Pb coverage, they identified both substrate- and adsorbate-induced features, and therefore ruled out that the pattern with three protrusions per unit cell, as seen by Hwang and Golovchenko, matches the arrangement of the adsorbed Pb atoms. Their measurements illustrate the fact that it is generally not possible to obtain reliable structural information on the basis of STM data alone.

C. 1×1 phase: a two-dimensional solid or liquid?

For the same Pb coverage, we have heated the substrate to 260 °C, well above the transition temperature to the 1×1

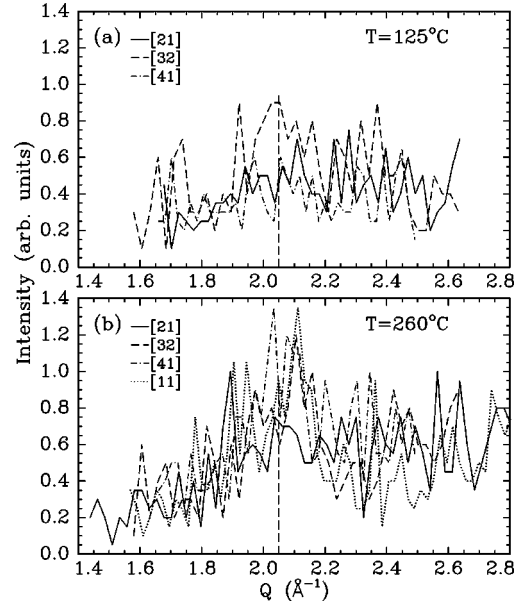


FIG. 5. Radial scans in the directions $[hk]=[21]$, $[32]$, $[41]$, and $[11]$ (a) below and (b) above the phase transition. In (a) the $[11]$ direction is omitted, because of the huge $(\frac{2}{3}\frac{2}{3})$ peak at $Q=2.09$ Å⁻¹. The dashed line marks $Q=2.05$ Å⁻¹ where Grey *et al.* (Ref. 17) found the maximum of the diffraction ring.

phase. We have confirmed the observation of Grey *et al.*¹⁷ that a diffraction ring appears, characteristic of a two-dimensional liquid phase. Radial scans perpendicular to this ring in the directions $[hk]=[21]$, $[32]$, $[41]$, and $[11]$ are shown in Fig. 5. Although the count rates are very low in these scans (the beam conditions were not optimal), at a temperature of 260 °C the appearance of the ring of diffuse scattering is visible [Fig. 5(b)]. It is hard to obtain the peak width and position of the ring, but the peak position we find is very close to the position reported by Grey *et al.* at $Q=2.05$ Å⁻¹, which is marked by the dashed line in the figure. This diffuse ring of scattering is thus evidence that the Pb monolayer indeed behaves partly as a two-dimensional liquid. For a genuine two-dimensional liquid, the value of 2.05 Å⁻¹ corresponds to a nearest-neighbor distance of 3.42 Å.¹³

Figure 6 shows the distribution of measured structure factors along the (0 1) and (0 2) rods for this phase (filled circles) together with the data for the β phase (open circles). The effect of the phase transition on the (0 1) rod is hardly visible, while the change in the (0 2) rod is more dramatic. The dashed curve is a calculation for a simple bulk-terminated Ge(111) crystal (unreconstructed), and for the (0 2) rod the measured structure factors follow this curve quite well. This rod is very sensitive to the $(\sqrt{3}\times\sqrt{3})R30^\circ$ structure, and above the transition there seems to be no ordered Pb visible at all. Apparently, the Pb layer has both liquidlike and solidlike properties. Next we will quantify this by discussing various models of the high-temperature phase.

There are two types of models: one with a $(\sqrt{3}\times\sqrt{3})R30^\circ$ unit cell and vanishing correlation length, the other with a genuine 1×1 cell. The liquid ring or the vanishing correlation lengths point to a high mobility. For this reason, we assume the surface to be uniform (i.e., the surface fraction equals 1) and allow for coverages below $\frac{4}{3}$ ML by

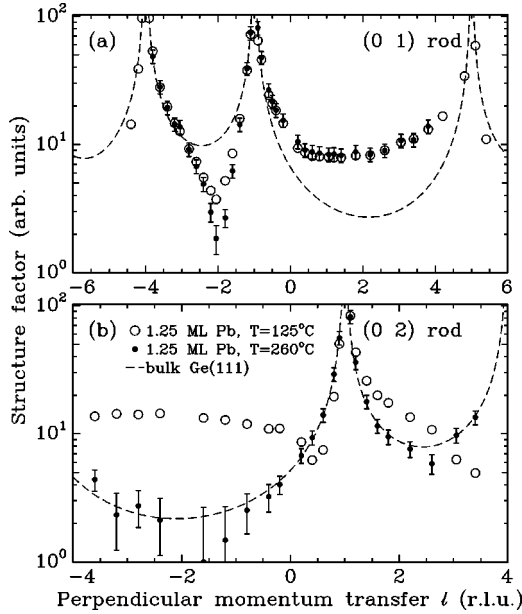


FIG. 6. Structure factors along the (01) and (02) crystal truncation rods. Measured structure factors are indicated by open circles for the β phase at 125 °C, and filled circles represent the data for the 1×1 phase at 260 °C. The dashed curves give calculations for the flat bulk-terminated Ge(111) surface.

varying the occupancies of the different possible sites. We start our analysis by taking a 1×1 unit cell and allowing the Pb atoms to occupy any of the three high-symmetry sites T_1 , T_4 , or H_3 on the surface. When we do our fit procedure we find that the T_4 site is not significantly occupied (less than 15%), and therefore we do not consider this position any further. This is consistent with the low-temperature model and the conclusions of others.^{23,26} When we allow only the T_1 and H_3 sites we find in our best-fit model that the T_1 site is 89% occupied and the H_3 site 29% (see Table II, column “ 1×1 ”; and Fig. 7, solid curve). This corresponds to a total coverage of 1.17 ML, consistent with our estimated Pb coverage of 1.25 ML. In molecular-dynamic simulations done in Ref. 23, it was proposed that the Pb overlayer becomes diffusive above the phase transition, but that the Pb atoms still

TABLE II. Best-fit parameters, reduced χ^2 values, and Pb nearest-neighbor distances for the structural models for the high-temperature 1×1 phase of 1.25-ML Pb on Ge(111). Fixed values are indicated by an asterisk (*). The 1×1 model is equivalent to the model proposed by Franklin *et al.* (Ref. 26) (see text).

Fit parameter	1×1	β model	β fit	Trimer
In-plane displacement (\AA)	0*	0.39*	0.83	0.50
Height H_3 atom (\AA)	2.90	2.88*	2.91	2.93
Height (OC) T_1 atoms (\AA)	2.70	2.76*	2.72	2.76
H_3 occupancy	0.29	0.59	1*	0.51
(OC) T_1 occupancies	0.89	1	1*	0.59
Debye-Waller B_{par} (\AA^2)	35	24	35	6.3*
Debye-Waller B_{perp} (\AA^2)	1	1	1	1*
χ^2	0.3	2.4	0.3	0.7
Pb nearest-neighbor distance (\AA)	2.32	3.07	2.65	1.82

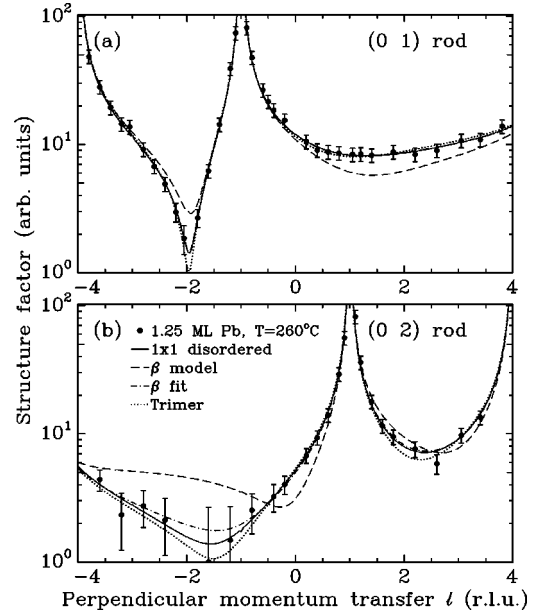


FIG. 7. Structure factors along the (01) and (02) crystal truncation rods at a substrate temperature of 260 °C. Measured structure factors are indicated by filled circles. The curves are model calculations (see text).

spend an important fraction close to symmetry sites. The average time spent close to a T_1 site was 58%, close to a T_4 site 14%, and close to an H_3 site 28%. They showed that the diffusion in the overlayer is not purely two-dimensional liquidlike, but has lattice-gas-like features. These calculations were done for a higher temperature, and the authors of Ref. 23 speculated that for temperatures around ~ 200 °C the non-liquid-like features should be comparatively more important. This is consistent with our observations.

Hwang and Golovchenko²¹ proposed that at the phase transition the long-range order of the $(\sqrt{3} \times \sqrt{3})R30^\circ$ reconstruction is destroyed by thermal fluctuations. The $(\sqrt{3} \times \sqrt{3})R30^\circ$ domains become very small, but in principle the structure stays the same. Since we have shown that their trimer model is not consistent with our data, we have tried to fit our high-temperature data with our structural model for the β phase. In its extreme form, this model would predict the $(\sqrt{3} \times \sqrt{3})R30^\circ$ reflections to disappear while the integer-order ones remain constant, because these are insensitive to the antiphase domain disorder. The data in Fig. 6 show that this is not true. So instead we tried to fit the high-temperature data keeping the displacements fixed and varying only the occupancies and Debye-Waller parameters. We do not find a good fit to our data in this way (see Table II, column “ β model”; and Fig. 7, dashed curve).

Thus during the phase transition, some of the structural parameters vary. If we fit the displacements in the β -phase model we obtain a fit to our data that is as good as the 1×1 fit (see Table II, column “ β fit”; and Fig. 7, dash-dotted curve). The OC T_1 atoms are displaced much closer to the T_1 sites than in the low-temperature β phase. If the in-plane displacement equals 1.15 \AA , the atoms are exactly on T_1 sites. This is the model proposed by Franklin *et al.*,²⁶ who suggested that at the phase transition the symmetry of the ideal Ge(111) surface is thus restored. For the integer-order

rods we can measure, this model gives the same results as the 1×1 model, because for these rods one site out of three that is fully occupied in a $(\sqrt{3} \times \sqrt{3})R30^\circ$ unit cell is equivalent to all sites with a $\frac{1}{3}$ occupancy.

The in-plane Debye-Waller parameter B_{par} of 35 corresponds to an in-plane rms vibrational amplitude of 0.67 Å. Franklin *et al.* found an in-plane rms vibrational amplitude of 0.60 Å. These vibrational amplitudes are huge, although consistent with the greatly agitated state of the Pb atoms seen in STM pictures²¹ and with molecular-dynamics calculations.²³ Unfortunately, we only have two complete CTR's, so we cannot observe the effect of the Debye-Waller factor over a large range in parallel momentum transfer. To see whether it is possible to find a good fit to our data without the large vibrational amplitudes, we tried several models while fixing the Debye-Waller parameters to the values found for the β phase. Note that from the Debye temperature $T_D \sim 55$ K mentioned above, the temperature rise from 125 to 260 °C should result in an increase of $\sqrt{\langle u^2 \rangle} = 0.30$ Å to 0.35 Å. The only model for which we obtain a good fit to our data, is a model where trimers of atoms on T_1 sites are displaced toward the H_3 center by 0.5 Å. This model is similar to that proposed by Hwang and Golovchenko,²¹ except that we also have a Pb atom in the middle of the trimer at the H_3 site. The occupancies found for the two sites are 0.51 and 0.59 for the H_3 and T_1 sites, respectively (see Table II, column "Trimer"; and Fig. 7, dash-dotted curve) corresponding to a visible coverage of only 0.76 ML. The remaining 0.5 ML do not follow the Ge(111) lattice, and could therefore be liquid-like.

The models for the high-temperature phase all predict surprisingly small nearest-neighbor distances for the Pb atoms compared to the covalent distance of 2.94 Å. The 1×1 (and Franklin) model gives 2.32 Å, the β -fit model 2.65 Å, and the trimer model 1.82 Å. Differences in height cannot significantly change this. From our data we know for sure that the 1×1 phase has a different structure than the β phase, which *does* have the expected bond distance. The bond-length argument thus favors the β -fit model and essentially rules out the trimer model. The 1×1 model yields a 20% decrease in nearest-neighbor distance, which seems unlikely. A large change in bond distance is only expected if the phase transition simultaneously modifies the electronic structure.

On the basis of our data we cannot fully decide whether the 1×1 phase consists of very small domains of $(\sqrt{3} \times \sqrt{3})R30^\circ$ structure as proposed by Hwang and Golovchenko,²¹ or of an ordered phase where all Pb atoms occupy high-symmetry sites with a high diffusion between these sites, as was proposed in Ref. 23. When the domain size becomes very small, a large fraction of the Pb atoms is located at domain boundaries. This may lead to additional relaxations that we only model on average in the structure of our model unit cells.

The bond lengths favor the β -fit model, in which a snapshot would closely resemble the low-temperature structure shown in Fig. 4. The atoms on OC T_1 sites are in the β -fit model closer to the T_1 sites (see the "solid" Pb atoms in Fig. 8), which could well be caused by the fact that on average the number of nearest neighbors is reduced compared

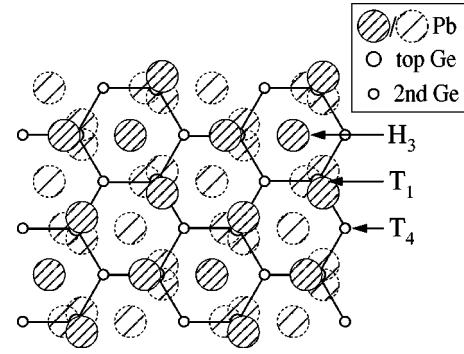


FIG. 8. Schematic top view of our " β -fit" structural model. The "solid" Pb atoms are placed in one $(\sqrt{3} \times \sqrt{3})R30^\circ$ domain, and can be considered as a snapshot of the surface. The "dashed" Pb atoms indicate the positions where the Pb atoms on average can also be found, forming other domains (see the text).

to the saturation coverage. Size hindrance prevents the atoms from occupying the exact T_1 sites. Because of diffusion, all atoms rapidly change positions, and on average all H_3 sites will have the same occupancy, while all three equivalent OC T_1 sites will also be equally occupied (see the "dashed" Pb atoms in Fig. 8). These occupancies are less than $\frac{1}{3}$, since the atoms can also be found on nonlattice sites, as evidenced by the liquid ring. The fact that the phase transition occurs for a coverage of 1.25 ML is consistent with this picture and points to a *lattice-gas* model. When more Pb atoms are added more sites are occupied and there is no room for diffusion left. Therefore, at a coverage of $\frac{4}{3}$ ML the Pb adlayer is forced to the $(\sqrt{3} \times \sqrt{3})R30^\circ$ reconstruction. This reconstruction melts at a temperature of ~ 330 °C, which is close to the bulk melting point of Pb of 327.5 °C.

IV. CONCLUSIONS

We have determined that the β phase has four atoms per unit cell, and therefore the saturation coverage is $\frac{4}{3}$ ML. Our model, consisting of three Pb atoms on OC T_1 sites and one Pb atom on an H_3 site, is consistent with other LEED and x-ray scattering studies.

The phase transition to the 1×1 phase was found to be an order-order transition, and disagrees with a strictly two-dimensional liquid interpretation. To explain our measurements, large in-plane thermal vibration amplitudes are required. The picture that emerges is that of rapidly diffusing atoms that spend a significant fraction of their time close to lattice sites. More theoretical work is necessary to reconcile this with the simultaneous observation of liquid diffraction rings.

ACKNOWLEDGMENTS

We thank Marc Langelaar, Willem Jan Huisman, Steve Bennett, and Erik van der Vegt for their help during the measurements. René Koper is acknowledged for polishing the Ge crystal. This work was part of the research program of the Foundation for Fundamental Research on Matter (FOM), and was made possible by financial support from the Netherlands Organization for Scientific Research (NWO).

- *Present address: European Synchrotron Radiation Facility, B.P. 220, 38043 Grenoble Cedex, France.
- †Author to whom correspondence should be addressed. FAX: +31.24.3653067. Electronic address: vlieg@sci.kun.nl
- ¹E. Bauser, in *Handbook of Crystal Growth*, edited by D. T. J. Hurle (Elsevier, Amsterdam, 1994), Vol. 3b, pp. 879–939.
- ²*Ordering in Two Dimensions*, edited by S. K. Sinha (Elsevier, New York, 1980).
- ³J. W. M. Frenken and H. M. van Pinxteren, in *Phase Transitions and Adsorbate Restructuring at Metal Surfaces*, edited by D. A. King and D. P. Woodruff, The Chemical Physics of Solid Surfaces, Vol. 7 (Elsevier, Amsterdam, 1994), pp. 259–290.
- ⁴P. H. Fuoss, L. J. Norton, and S. Brennan, Phys. Rev. Lett. **60**, 2046 (1988).
- ⁵H. M. van Pinxteren, S. Chandavarkar, W. J. Huisman, J. M. Gay, and E. Vlieg, Phys. Rev. B **51**, 14 753 (1995).
- ⁶J. J. Métois and G. Le Lay, Surf. Sci. **133**, 422 (1983).
- ⁷T. Ichikawa, Solid State Commun. **46**, 827 (1983).
- ⁸T. Ichikawa, Solid State Commun. **49**, 59 (1984).
- ⁹R. Feidenhans'l, J. S. Pedersen, M. Nielsen, F. Grey, and R. L. Johnson, Surf. Sci. **178**, 927 (1986).
- ¹⁰B. P. Tonner, H. Li, M. J. Robrecht, Y. C. Chou, M. Onellion, and J. L. Erskine, Phys. Rev. B **34**, 4386 (1986).
- ¹¹J. S. Pedersen, R. Feidenhans'l, M. Nielsen, K. Kjær, F. Grey, and R. L. Johnson, Surf. Sci. **189-190**, 1047 (1987).
- ¹²B. P. Tonner, H. Li, M. J. Robrecht, M. Onellion, and J. L. Erskine, Phys. Rev. B **36**, 989 (1987).
- ¹³F. Grey, Ph.D. thesis, Copenhagen University, 1988 (unpublished).
- ¹⁴B. N. Dev, F. Grey, R. L. Johnson, and G. Materlik, Europhys. Lett. **6**, 311 (1988).
- ¹⁵H. Li and B. P. Tonner, Surf. Sci. **193**, 10 (1988).
- ¹⁶H. Huang, C. M. Wei, H. Li, B. P. Tonner, and S. Y. Tong, Phys. Rev. Lett. **62**, 559 (1989).
- ¹⁷F. Grey, R. Feidenhans'l, J. Skov Pedersen, M. Nielsen, and R. L. Johnson, Phys. Rev. B **41**, 9519 (1990).
- ¹⁸M. Abraham and G. Le Lay, Thin Solid Films **233**, 264 (1993).
- ¹⁹F. Ancilotto, A. Selloni, and R. Car, Phys. Rev. Lett. **71**, 3685 (1993).
- ²⁰L. Seehofer, G. Falkenberg, and R. L. Johnson, Surf. Sci. **290**, 15 (1993).
- ²¹I.-S. Hwang and J. A. Golovchenko, Phys. Rev. Lett. **71**, 255 (1993).
- ²²I.-S. Hwang and J. A. Golovchenko, Phys. Rev. B **50**, 18 535 (1994).
- ²³F. Ancilotto, A. Selloni, and R. Car, Phys. Rev. B **50**, 15 158 (1994).
- ²⁴L. Seehofer, D. Daboul, G. Falkenberg, and R. L. Johnson, Surf. Sci. **307-309**, 698 (1994).
- ²⁵L. Seehofer, D. Daboul, G. Falkenberg, and R. L. Johnson, Surf. Sci. **314**, L879 (1994).
- ²⁶G. E. Franklin, M. J. Bedzyk, J. C. Woicik, Chien Liu, J. R. Patel, and J. A. Golovchenko, Phys. Rev. B **51**, 2440 (1995).
- ²⁷J. M. Carpinelli, H. H. Weitering, E. W. Plummer, and R. Stumpf, Nature (London) **381**, 398 (1996).
- ²⁸J. Avila, A. Mascaraque, E. G. Michel, and M. C. Asensio, Appl. Surf. Sci. **123/124**, 626 (1998).
- ²⁹K. Würde, P. Krüger, A. Mazur, and J. Pollmann, Surf. Rev. Lett. **5**, 105 (1998).
- ³⁰I. K. Robinson, Phys. Rev. B **33**, 3830 (1986).
- ³¹C. Norris, M. S. Finney, G. F. Clark, G. Baker, P. R. Moore, and R. van Silfhout, Rev. Sci. Instrum. **63**, 1083 (1992).
- ³²E. Vlieg, A. van 't Ent, A. P. de Jongh, H. Neerings, and J. F. van der Veen, Nucl. Instrum. Methods Phys. Res. A **262**, 522 (1987).
- ³³E. Vlieg, J. F. van der Veen, J. E. Macdonald, and M. Miller, J. Appl. Crystallogr. **20**, 330 (1987).
- ³⁴E. Vlieg, J. Appl. Crystallogr. **30**, 532 (1997).
- ³⁵R. Feidenhans'l, Surf. Sci. Rep. **10**, 105 (1989).
- ³⁶E. Vlieg, J. F. van der Veen, S. J. Gurman, C. Norris, and J. E. Macdonald, Surf. Sci. **210**, 301 (1989).
- ³⁷R. Feidenhans'l, J. S. Pedersen, J. Bohr, M. Nielsen, F. Grey, and R. L. Johnson, Phys. Rev. B **38**, 9715 (1988).
- ³⁸R. G. van Silfhout, J. F. van der Veen, C. Norris, and J. E. Macdonald, Faraday Discuss. Chem. Soc. **89**, 169 (1990).
- ³⁹B. W. Batterman and D. R. Chipman, Phys. Rev. **127**, 690 (1962).
- ⁴⁰B. E. Warren, *X-Ray Diffraction* (Addison-Wesley, Reading, MA, 1969).
- ⁴¹B. N. Dev, Phys. Rev. Lett. **64**, 1182 (1990).